

See discussions, stats, and author profiles for this publication at: <https://www.researchgate.net/publication/321429756>

Non-standard patterns for gridshells: fabrication and structural optimization

Article in Journal of the International Association for Shell and Spatial Structures · December 2017

DOI: 10.20898/j.iass.2017.194.893

CITATIONS

17

READS

1,497

3 authors, including:



Romain Mesnil

École des Ponts ParisTech

53 PUBLICATIONS 350 CITATIONS

SEE PROFILE



Olivier Baverel

École des Ponts ParisTech

196 PUBLICATIONS 1,720 CITATIONS

SEE PROFILE

Some of the authors of this publication are also working on these related projects:



Generative design of interlocked assemblies [View project](#)



Elastic gridshells [View project](#)

NON-STANDARD PATTERNS FOR GRIDSHELL STRUCTURES: FABRICATION AND STRUCTURAL OPTIMIZATION

Romain MESNIL¹, Cyril DOUTHE¹ and Olivier BAVEREL^{1,2}

¹ Laboratoire Navier, UMR 8205, Ecole des Ponts, IFSTTAR, CNRS, UPE, Champs-sur-Marne, FRANCE

² Laboratoire GSA, ENSA, Grenoble, FRANCE

Editor's Note: The first author of this paper is one of the four winners of the 2017 Hangai Prize, awarded for outstanding papers that are submitted for presentation and publication at the annual IASS Symposium by younger members of the Association (under 30 years old). It is re-published here with permission of the editors of the proceedings of the IASS Symposium 2017: "Interfaces –Architecture. Engineering. Science" held in September 2017 in Hamburg, Germany.

DOI: <https://doi.org/10.20898/j.iass.2017.194.893>

ABSTRACT

The design of gridshells is subject to strong mechanical and fabrication constraints, which remain largely unexplored for non-regular patterns. The main technological constraints for glazed gridshells are related to the planarity of facets and the existence of torsion-free offsets. The authors propose indicators to evaluate a priori the quality of design space of gridshells covered with different patterns for these fabrication constraints. By comparing these metrics, the kagome grid pattern is identified as a pattern with a complexity similar to the ubiquitous quadrilateral pattern. Finally, the authors propose to generate gridshells with planar facets with the marionette technique and to explore the resulting design space by the means of multi-objective optimization. The results of the study show that our framework for shape modeling has similar performances as more usual frameworks, like NURBS modeling, while maintaining the facet planarity.

Keywords: Structural morphology, multi-objective optimization, conceptual design, gridshell, marionette mesh, PQ-mesh, kagome

1. INTRODUCTION

1.1. Morphogenesis of gridshell structures

The construction of doubly curved structures is characterized by the compromise made by the architect and the structural engineer between the respect of design intent, the structural reliability and the constructability of the envelope and structure. This interaction between technology, structure and geometry is the purpose of structural morphology [1]. Such interplay is particularly important in the case of glazed gridshells, where structural pattern and envelope are strongly interdependent.

Jörg Schlaich and Hans Schober [2] identified the planarity of glass panels as one of the key aspects in the economy of gridshells and proposed surfaces of translations and scale-trans surfaces to generate gridshells with planar quadrilateral facets. The second key technological constraint, represented in Figure 1, is to build with so-called torsion-free nodes, to fabricate planar beams whose planes of

symmetry intersect a common node axis. Such configurations cannot be obtained for triangulated gridshells, besides "trivial" offsets [3] (e.g. extrusion of the sections in the vertical direction). On contrary, quadrilateral meshes can yield non-trivial offsets, where the nodal axes are close to the normal vectors of the underlying smooth surface.



Figure 1: A node with torsion (picture: Romain Mesnil)

1.2. Previous work on gridshells with non-regular grid patterns

The constructability of non-regular grids (node offset and planarity of panels) as well as their mechanical performance are rarely studied, with a few notable exceptions [4]. Perhaps the most notable example of irregular gridshell structure is the roof over the court of the Maritime Museum in Amsterdam, which is a funicular shape covered with planar facets [5]. The planarity of the facets was obtained by the computation of a Maxwell reciprocal diagram of the grid pattern. The basis pattern is shown in Figure 2.

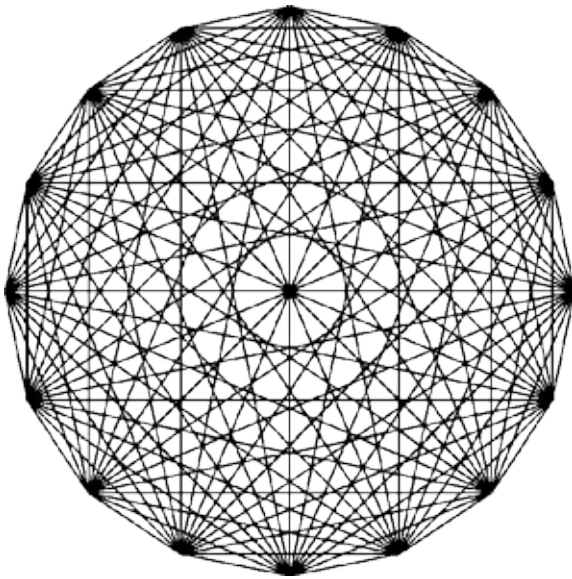


Figure 2: Grid pattern used as a basis for the Dutch Maritime Museum [5]

1.3. Research statement

The morphogenesis of gridshells is usually governed by fabrication constraints, like facet planarity or the construction of torsion-free nodes [6]. The triangular and quadrilateral patterns, which have been used preferably by architects and engineers, have both limitations. The exploration of less common pattern could provide designers with better design spaces for glazed gridshells, both from constructional and mechanical perspective. The objective of the present paper is therefore to provide a framework to design gridshells with non-regular patterns. The contributions are of increasing complexity, corresponding to different design stages.

First, we present simple indicators that can be used during conceptual design stages that inform the designer on the quality of a pattern for planarization or the construction of torsion-free nodes. Then, we propose a reconciliation of structural optimization and geometrically-constrained design approach. Like proposed by Borgart [7], we embed a fabrication-constraint, namely facet planarity, within the description of the design space and perform optimization under feasibility constraint. The possibilities of the proposed framework are demonstrated through a detailed study on the kagome grid pattern, which is made of hexagons and triangles, in the following of [8].

2. METHODOLOGY

2.1. Shape modeling with the marionette technique

In the following, we represent a gridshell by a mesh, whose edges correspond to the neutral axes of the beams of the gridshells. We write n_v , n_e and n_f the number of vertices, edges and faces respectively. This paper proposes to model complex shape with the aid of the marionette technique, already proposed by the authors in [9] and illustrated in Figure 3. The method is based upon the prescription of a plane-view of a quad mesh. The planarity of a quad $ABCD$ is measured by the nullity of the determinant. Using the notation $\mathbf{x}_{AB} = \mathbf{x}_B - \mathbf{x}_A$, we have:

$$\det(\mathbf{AB}, \mathbf{AC}, \mathbf{AD}) = (x_{AB}y_{AC} - x_{AC}y_{AB})z_{AD} + (x_{AD}y_{AB} - x_{AB}y_{AD})z_{AC} + (x_{AC}y_{AD} - x_{AD}y_{AC})z_{AB} = 0 \quad (1)$$

Obviously, this equation is linear in z_{AB} , z_{AC} and z_{AD} . Once the projection in the (xy) plane is chosen, the determination of a planar quad can thus be interpreted as a linear constraint. From a practical point of view, in a quad mesh, the end user controls a plane view and several elevation curves, and uses thus features of descriptive geometry, which are well known by engineers and architects. The parameterization of the plane-view with Bézier surfaces and of elevation curves with splines provides an interesting CAD-based modeling approach that could be used as an alternative to NURBS surfaces. The performance of this approach for the shape optimization of shell structures was proved promising in [10].

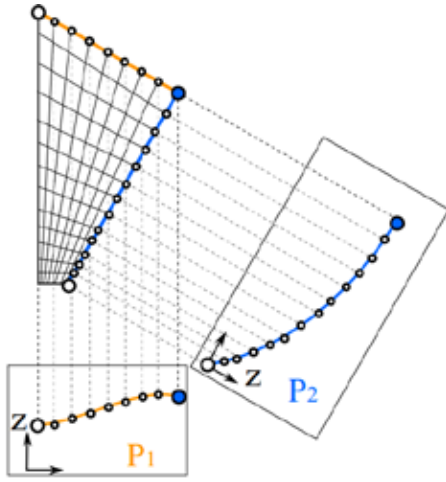


Figure 3: A unique PQ-mesh can be determined from a planar projection and two elevations [10]

We propose to extend the marionette technique to non-regular meshes. A polygon with n facets is planar if and only if $(n - 3)$ consecutive sets of four vertices are co-planar. The marionette lifting of a planar quad being governed by a linear constraint recalled in equation (1), the determination of a planar n -gon can be interpreted as $(n - 3)$ linear constraints, and the space of solutions for the marionette lifting of any mesh is thus a vector space. A basis of this vector space can be computed using Singular Value Decomposition, similarly to the method for exploration of PQ-mesh deformations with affine maps by Vaxman[11].

2.2. Constructability assessment

2.2.1. Motivation

The generation of meshes covered with planar facets or of torsion-free beam layouts has been the subject of numerous developments in the recent years. Rather than focusing on an algorithmic point of view on these problems, we propose here to analyze the size of the design space of feasible solutions for each pattern. The understanding of the construction of feasible subspaces with the marionette technique, or with so-called Combescure transformations, allows indeed providing two metrics that inform the designers on the potential offered by regular or non-regular patterns in terms of fabrication.

2.2.2. Size of the design space for facet planarity

The size of the design space offered by the marionette technique was computed in [9]. Consider first the size of the design space for a mesh with

planar facets. Each vertex of a mesh has 3 degrees of freedom, and for a face with N vertices, the planarity implies $(N-3)$ constraints. Indeed, once three points of a face are chosen, they define a plane and the $(N-3)$ remaining vertices are constrained to be on the created plane. The size of the design space is thus:

$$d = 3n_v - \sum_{Facets} (N - 3) \quad (2)$$

With the marionette technique, the in-plane view is considered as an input. The vector space of solutions has thus a dimension given by equation (3):

$$d_{Marionette} = n_v - \sum_{Facets} (N - 3) \quad (3)$$

In the followings, we nonetheless use the metric defined by equation (2), since the plane view can be modified before marionette lifting. We also point out that the method described in [12] could be used to generate exact PQ-meshes, but that a meaningful basis of the space of solutions is not immediate.

2.2.3. Size of the design space for offsets

The existence of torsion-free nodes is linked to the construction of so-called *parallel meshes* [3]. Two meshes are said to be parallel if they have the same connectivity and their respective edges are parallel. Consider Figure 4, which displays two parallel meshes M and M' : it is clear that the surfaces spanning between two parallel edges (highlighted in blue) are planar. Therefore, the line linking the respective vertices of two parallel meshes are axes of torsion-free beam layouts.

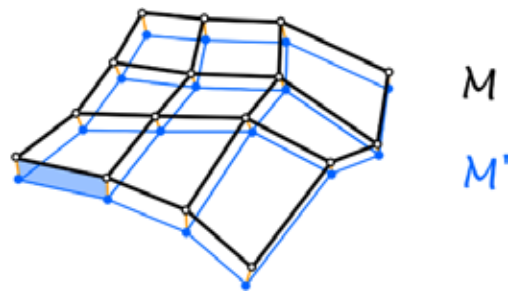


Figure 4: Two parallel meshes and the corresponding planar beam layout

Two parallel meshes are related by a *Combescure transformation*. It was shown in [3] that Combescure transformations depend linearly on the coordinates of the vertices, so that the space of parallel meshes is a linear space. Pottmann *et al.* [3] estimated the size of the design space as follows: each edge can change its length, but for a given facet with N edges, only

(N-2) edges can be chosen independently. The size of the design space is thus given by:

$$d_{Combescure} = n_e - 2n_F + 3 \quad (4)$$

2.2.4. Funicular shapes and mesh parallelism

Combescure transformations are closely related to the study of funicular shapes and appear naturally in the context of Thrust Network Analysis[13].

Consider a planar form diagram, like the one depicted in black in **Figure 5**. A state of self-stress can be constructed if a reciprocal force-diagram exists. For a prescribed form diagram, the statically compatible self-stresses define a linear space, which is invariant by parallel transformations of the dual force-diagram.

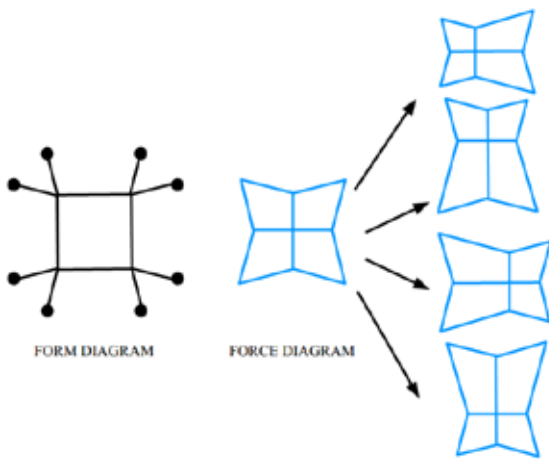


Figure 5: Form-force reciprocal diagrams: applying a Combescure transformation to the force diagram leaves the force diagram invariant

Denoting n_e^* and n_F^* the number of edges and faces in the dual force-diagram, the dimension of the space of states of self-stress of a given form diagram is found by applying equation (3):

$$d_{Self-stress} = n_e^* - 2n_F^* + 3 \quad (5)$$

Thus,

$$d_{Self-stress} = n_e - 2n_V + 3 \quad (6)$$

We point out a link between equation (6) and the extended Maxwell's rule, which counts the mechanisms m and states of self-stress s of planar truss [14]. A simple relation involving Euler's characteristic χ of the mesh relates hence equations

(3) and (6): the sum of $(s - m)$ and $d_{Combescure}$ is thus a topological constant of the mesh.

$$(s - m) + d_{Combescure} = -2 \cdot \chi + 6 \quad (7)$$

In equation (3) and (4), the constants correspond to rigid body motion and can be discarded. The interest of studying states of self-stress of planar graphs has been highlighted in [15].

Therefore, grid patterns that offer a wide variety of states of self-stress and a rich design space for funicular shapes also offer few degrees of freedom in terms of offset with torsion-free nodes.

2.3. Structural performance assessment

2.3.1. Homogenization and parametric studies

An interesting approach to evaluate the quality of a pattern is to compute a homogenized shell behavior. The method, which can be applied to periodic structures only, computes an equivalent stiffness tensor of a plate. It has been applied to gridshells with various plate or shell models: [17] considered orthotropic Love-Kirchhoff models while [18] considered an enriched model considering shear deformations. While detailed structural analysis is required to assess the buckling of a gridshell, homogenization gives precious information on the relative stiffness of different patterns, without getting involved in heavy finite element computations. This approach has been used and validated with a comparison to the results of a parametric study in [8].

2.3.2. Structural exploration by multi-objective optimization

In advanced design stage, the use of more sophisticated modeling tools is required. We propose to parameterize the design space with the Marionette technique and to analyze the linear buckling of gridshells. The parameterization of the marionette design space with few degrees of freedom, in the manner of NURBS has been proposed by the authors in [10] and applied to the shape optimization of shell structures. In real-life projects, the designer aims at conciliating possibly competing optimization objectives, like the mass of the structure and the number of bars to assemble. In the following of [19], we use thus a multi-objective optimization algorithm to explore the possibilities of the design spaces

offered by different patterns. The software used in this study is the Grasshopper plug-in *Octopus*.

3. A PRIORI COMPARISON OF DESIGN SPACES

3.1. Comparisons

For the sake of brevity, we consider only a few patterns that occur in existing literature on the modeling of polyhedral meshes [16], or in built projects. We set particular emphasis on periodic patterns, which are suited for homogenization and which constitute already a subset of patterns which has rarely been applied to gridshell structures besides triangular and quadrilateral pattern. For reference, we also include a pattern derived from the Petrie polygon of the simplex in 15 dimensions shown in Figure 2, which was used for the courtyard of the Dutch Maritime Museum.

The performance metrics computed in equations (3), (4) and (5) depend on the number of edges or vertices in the meshes. In the followings, we present normalized values that constitute our performance indicators: the higher their values, the richer the design space.

$$\begin{cases} d_{planarity} = \frac{d}{3n_v} \\ d_{offset} = \frac{d_{Combesure}}{n_e} \end{cases} \quad (8)$$

The indicators are computed for a periodic cell, with the assumption that other identical cells surround it. This point of view is in the spirit of homogenization, and it has to be noticed that it does not consider the boundaries of the meshes. Writing v_i and e_i the number of shared faces by the vertex (resp. the edge)

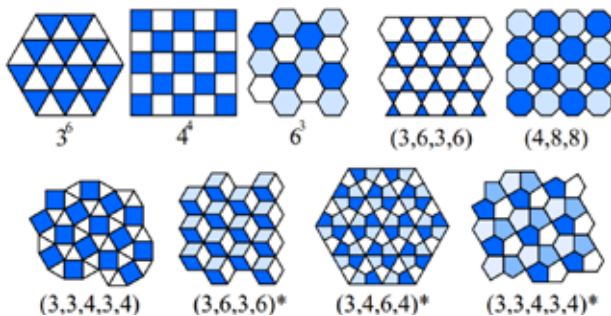


Figure 6: Periodic patterns studied in this paper and their vertex configuration (stars indicate dual patterns)

of index i , the indicators used in equation (7) should be computed with the n_v and n_e computed in equation (8).

$$\begin{cases} n_v = \sum_{Vertices} \frac{1}{v_i} \\ n_e = \sum_{Edges} \frac{1}{e_i} \end{cases} \quad (9)$$

3.2. Results

The computation of the performance indicators is thus conducted based on equations (7) and (8), and are summed up in Figure 7. It appears that the different patterns are scattered along a curve that illustrates the compromise that face designers. Some patterns (in dark on the Figure) have few degrees of freedom for planarity but the highest performance indicator for offsets, like the hexagonal pattern. Others (in light blue on the Figure) have many degrees of freedom for planarity of facets but no non-trivial offsets, like the triangular mesh. The indicator for the offsets is negative, which shows that the only possible offsets are the trivial ones (e.g. vertical extrusion of the members). Finally, a family of meshes, like quadrilateral meshes, is between these two extremes, and has an interesting potential for design explorations. Recall that because of equation (5), the size of the design space offered by TNA is the opposite of the one of the offsets. The consequence is that patterns suited for explorations with planar facets are also suited for explorations with funicular structures.

A gridshell based upon the 15-Polytope, like the gridshell covering the courtyard of the Dutch Maritime Museum, is revealed to offer much more degrees of freedom in terms of planarity than a quadrilateral mesh. The planarity indicator is indeed similar to the one of the snub square tiling, which seems intuitively relatively easy to planarize. On the other hand, this pattern offers no flexibility for the computation of torsion-free offsets, so that only a vertical offset is feasible with no nodal torsion. The converse observation is that this pattern offers many degrees of freedom for the manipulation of a force diagram in TNA. The cartography reveals thus that the pattern is indeed full of potential for the design methodology adopted in [5].

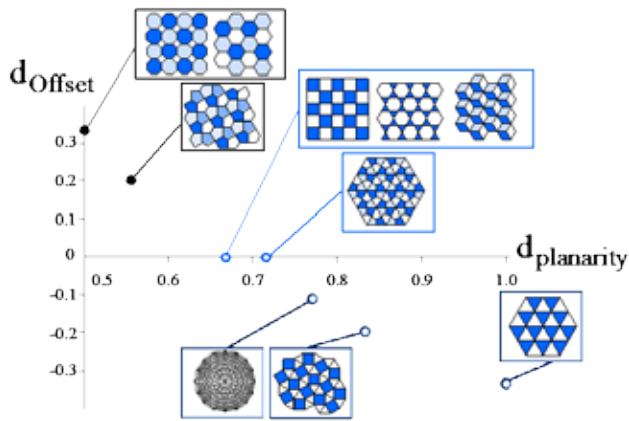


Figure 7: Classification of patterns with respect to fabrication constraints

3.3. Choice of a pattern

From our cartography, two patterns show performance indicators similar to the quadrilateral grid pattern: the kagome and the dual-kagome. This is in accordance with previous work, for example [9], which shows how to lift these meshes with the marionette technique in the manner of quad meshes. This offers a good point of comparison, as the quadrilateral grid pattern has been used extensively in built projects, and has been the object of parametric studies assessing its performances. In the followings, we focus on the kagome grid pattern, because all the nodes have a valence of four, so that their constructional complexity is indeed very similar to the one of quadrilateral grids.

4. APPLICATION: SHAPE OPTIMIZATION OF GRID SHELL STRUCTURES

4.1. Parameterization

In the followings, we consider the multi-objective optimization of a dome structure with the kagome grid pattern. We also compare two shape parameterizations: one with NURBS patches and one with Marionette patches, which yields planar facets automatically. A comparative study between kagome and quad pattern is also proposed for the NURBS model, so that 3 different parametric design spaces are compared:

- Marionette mesh with the kagome grid pattern
- NURBS with the kagome grid pattern
- NURBS with the quadrilateral grid pattern

The dome has a span of 40 meters, and is supported on an elliptical plane view. Due to symmetry, the shape is parameterized with 9 degrees of freedom for the NURBS model and 8 degrees of freedom for the Marionette model. A more detailed discussion on this parameterization for the shape optimization of shell structures is proposed in [20].

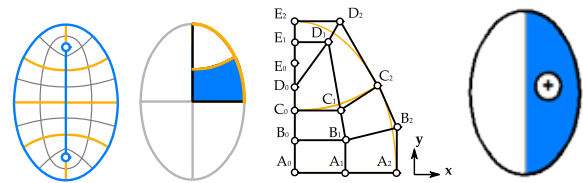


Figure 8: Left: parameterization of a dome with NURBS patches, right: load distribution of non-symmetrical load

The beams are rectangular hollow sections with $b/h=3$ and $t=1\text{cm}$. The height of the beams is restricted to 21cm. The number of beams is also a design variable. Due to the mesh topology, three subdivision parameters are used. The different parameters used in the present study are presented in Figure 9. There are respectively 12 and 13 optimization variables for the Marionette and NURBS design spaces.

Two load cases are considered in our study. First, we consider the self-weight of the cladding (set to 0.5kN/m^2) to which we add the self-weight of the structure (Load Case 0). The second load case (LC 1) is a non-symmetrical load applied vertically, which could correspond to an accumulation of snow. The load is applied to one half of the structure, as shown in Figure 8 (right), the amplitude of the load is set to 2kPa .

4.2. Optimization objectives and constraints

Mathematically, an optimization problem is written as the minimization of a quantity under constraints.

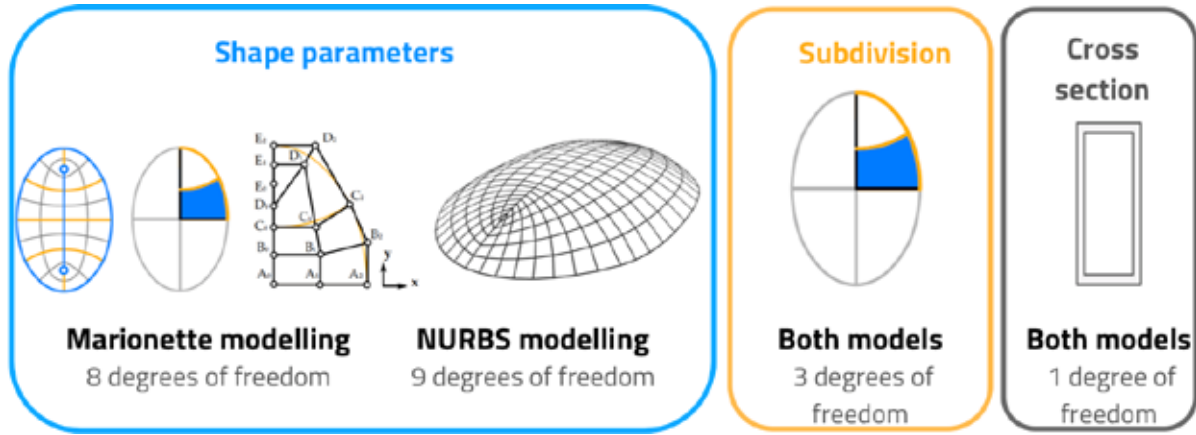


Figure 9: Parameters used for the optimization

$$\min_{\substack{f(x) \\ \text{subject to} \begin{cases} g_i(x)=0 \\ h_i(x)<0 \\ x_{L,i}<x_i<x_{U,i} \end{cases}}} f(x) \quad (10)$$

A designer usually aims at different objectives, of which we identified:

- The minimization of the structural mass
- The minimization of the glazed area (non-structural mass)
- The minimization of the number of connections.

The optimization is done under equality constraints, like the planarity of facets, which is expressed by equation (1). In our framework, the planarity constraint is directly taken into account in the definition of the design variables.

Structural optimization is often made under the assumption that the structure satisfies ultimate limit states and serviceability limit states. We use thus constrained optimization, and set three hard constraints:

- The maximal displacement under combination LC0+LC1 is inferior to $L/300$;
- The factor for linear buckling is superior to 10 for the combination $1.35LC0+1.5LC1$, as prescribed by EC3;
- 95% of the elements should have a stress inferior to the design stress according to EC3 under the combination $1.35LC0+1.5LC1$.

Constraints linked to the fabrication of elements are also added as hard constraints.

- The average length of the members is bounded between 1.2m and 2m.
- The standard deviation of the edge length has to be inferior to 0.3m.

4.3. Results

4.3.1. Discussion

The Pareto front computed for a population of 500 individuals per generation after 75 generations for the different design spaces is shown in Figure 10 and Figure 11. The Pareto fronts are in accordance with general considerations for the design of shells. Consider first that the surface area is proportional to the rise of the structure. Increasing the rise-over-span ratio usually improves the structural response of a shell: so it is logical that the Pareto fronts show this trend on the left hand side in Figure 10.

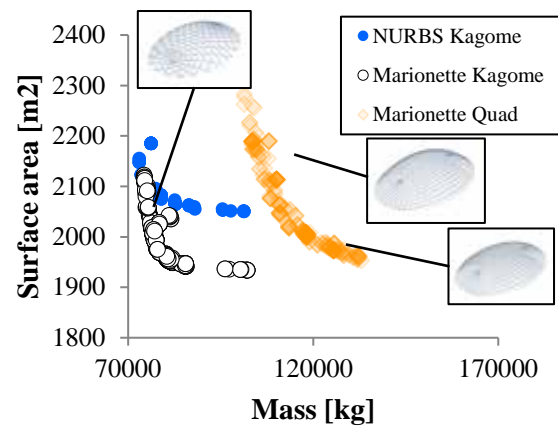


Figure 10: Pareto front after multi-criteria optimization with some optimal designs in the (Area,mass) objective space

It can be seen that the number of nodes (and beams) increases when the surface area decreases in Figure 11. Again, because shallow shells are less efficient, the loss of geometrical stiffness is compensated by a densification of the grids.

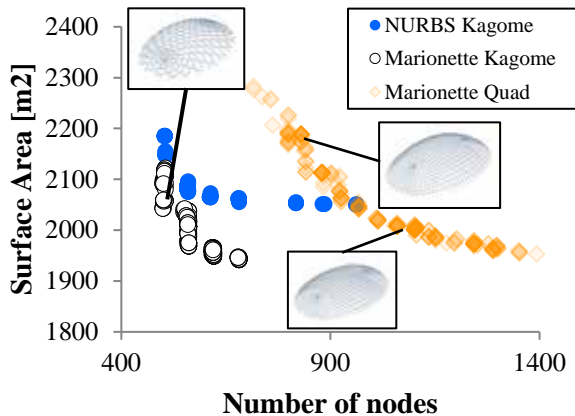


Figure 11: Pareto front after multi-criteria optimization with some optimal designs in the (Area, Nodes) objective space

4.3.2. Relative performance of marionette and NURBS design space for the Kagome grid pattern

Our study shows few differences between the Pareto fronts computed in the NURBS or Marionette design space. The lightest structure is found in the NURBS design space, but the difference between the mass of optima in the NURBS and Marionette design space is less than 5%, which demonstrates that the Marionette design space is suited for the parameterization of structural optimization for gridshell structures. It can be seen in Figure 10 that the optima of the marionette design space have a lower surface area

4.3.3. Relative performance of Kagome and quad pattern

The differences between optimization with kagome grid pattern and the quadrilateral grid pattern are much more important. The optima of PQ gridshells are clearly dominated by the ones of PK gridshells. Indeed, the mass of quadrilateral gridshells found by optimization is approximately higher by 30%, with respectively 101 tons and 75 tons for the Quad and Kagome design space. This is in accordance with a parametric study on the relative performances of the two grid patterns [8]. It can be noticed also that optima of quadrilateral gridshells feature 60% more beams or connection details, and should thus be expected to be more expensive. Notice that the Kagome and quadrilateral grid patterns shown in Figure 13 are covered with planar facets with the Marionette method.

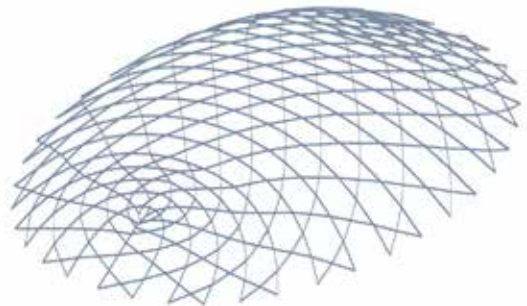


Figure 12: An individual of the Pareto front with the kagome grid pattern with the Marionette parameterization (The gridshell can be covered with planar facets)

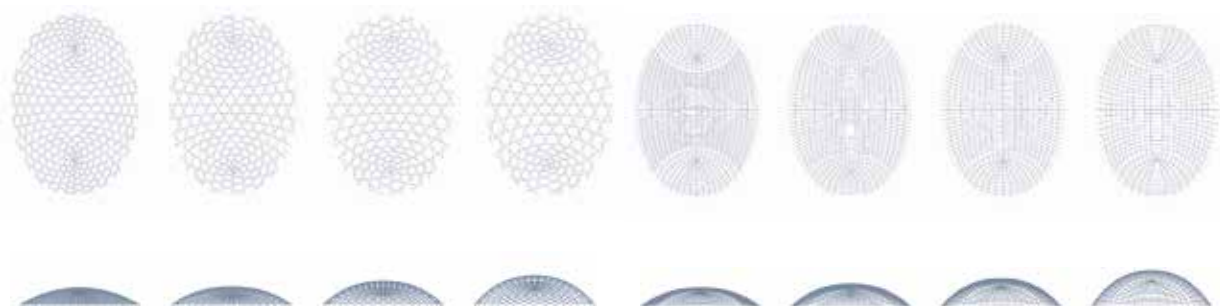


Figure 13: Several optima in the Marionette Design space: shallow structures are heavier and feature more nodes, the Kagome grid pattern yields better results for our performance metrics

4.4. Limitations of our study

It is a well-known fact that gridshell structures are buckling sensitive, and that their design is often governed by nonlinear criteria. In our study, the design criteria are treated as hard constraints. It appears that buckling is always the governing issue in our structures (the optima on the Pareto front have a linear buckling load factor close to 10). Note that we considered a simplified analysis scheme (perfect structure, linear buckling analysis and rigid nodes), which is far from conservative. In conceptual design, our modeling assumptions can be acceptable because the designer should not be expected to spend much time on modeling. In detailed design, more complex analysis involving geometrical and material nonlinearities, as well as nodal and geometrical imperfections should be made to validate the preliminary studies.

As gridshells with the kagome grid pattern have been found to be more sensitive to geometrical imperfections than quadrilateral gridshells, the relative performances of the kagome and quadrangular gridshells should thus be further studied with more in-depth analysis.

5. CONCLUSION

The design of doubly-curved structures challenges architects, engineers and builders. Usual grid patterns, like triangular and quadrilateral patterns for gridshells are well understood both in terms of constructability and structural performance. This article proposed a methodology to assess and explore design spaces offered by non-standard patterns. First, the authors proposed simple metrics to evaluate the dimension of the design space with different fabrication constraints. Second, the marionette technique is proposed to generate non-standard patterns with planar facets. Finally, the multi-objective optimization of gridshells with planar facets was proposed. These tools of increasing complexity could be used in different design stages, and provide the designer with a growing understanding of the design he or she is proposing.

Besides, the authors believe that their contribution on structural optimization is echoing the reflections made by Borgart [7] on this topic. Structural optimization is a powerful tool that is rarely used in the construction industry. One of the main reasons is that the outcome is not necessarily constructible.

Including fabrication constraints in the description of the design spaces can extend the possibilities of structural optimization in practice. This paper also demonstrates the relevance of the marionette technique for shape parameterization of gridshells covered with planar facets in the context of structural optimization. Mechanically optimal solutions obtained with our method are also feasible designs and incorporate cost considerations, and yet are as efficient as solutions with no constructive rationality obtained with Bézier surfaces.

REFERENCES

- [1] **Motro R.**, Structural Morphology, *J. IASS*, 1993.
- [2] **Schlaich J. and Schober H.**, Glass Roof for the Hippo Zoo at Berlin. *Structural Engineering International*, 1997; 7(4);252-254.
[DOI: 10.2749/101686697780494581]
- [3] **Pottmann H., Liu Y., Wallner J., Bobenko A. and Wang W.**, Geometry of multi-layer freeform structures for architecture. *ACM Transactions on Graphics*; 2007; 26(3); 65.
[DOI: 10.1145/1276377.1276458]
- [4] **Malek S. and Williams C.** Structural Implications of Using Cairo Tiling and Hexagons in gridshells, in *IASS 2013. Beyond the Limits of Man*. 2013.
- [5] **Adriaenssens, S., Ney, L., Bodarwe, E., & Williams, C.** Finding the form of an irregular meshed steel and glass shell based on construction constraints, *Journal of Architectural Engineering*, 2012, 18(3), 206-213.
[DOI: 10.1061/(ASCE)AE.1943-5568.0000074]
- [6] **Schober H.** *Transparent Shells: Form, Topology and Structure*. John Wiley & Sons, 2015.
[DOI: 10.1002/9783433605998]
- [7] **Borgart A.** New challenges for the Structural Morphology Group. *J. IASS*, 2010, 51(3), 183-189
- [8] **Mesnil R., Douthe C., Baverel O. and Léger B.** Linear buckling of quadrangular and

- Kagome grids: a comparative assessment. *Engineering Structures*, 2017, 132(3), 337-348.
[DOI: 10.1016/j.engstruct.2016.11.039]
- [9] **Mesnil R., Douthe C. and Baverel O.** Marionette Meshes: modeling free-form architecture with planar facets. *International Journal of Space Structures*, 2017, 32(3-4).
[DOI: 10.1177/0266351117738379]
- [10] **Mesnil R., Douthe C. and Baverel O.** Structural exploration of a fabrication-aware design space with Marionettes Meshes, in *Proceedings of the IASS Annual Symposium 2016*.
- [11] **Vaxman, A.** Modeling polyhedral meshes with affine maps. *Computer Graphics Forum*; 2012; 31(5); 1647-1656.
[DOI: 10.1111/j.1467-8659.2012.03170.x]
- [12] **Vaxman A.** A Projective Framework for Polyhedral Mesh Modelling *Computer Graphics Forum*; 2014; 33(8); 121-131.
[DOI: 10.1111/cgf.12405]
- [13] **Block P. and Ochsendorf J.** Thrust Network Analysis: A New Methodology for Three-Dimensional Equilibrium. *J. IASS*; 2007; 48(3);167-173
- [14] **Calladine C.R.,** Buckminster Fuller's "tensegrity" structures and Clerk Maxwell's rules for the construction of stiff frames. *International Journal of Solids and Structures*, 1978; 14(2); 161-172.
[DOI: 10.1016/0020-7683(78)90052-5]
- [15] **Block P., Van Maele T.** Algebraic Graph Statics. *Computer-Aided Design*; 2014; 53; 104-116.
[DOI: 10.1016/j.cad.2014.04.004]
- [16] **Jiang, C., Tang, C., Vaxman, A., Wonka, P., and Pottmann, H.,** Polyhedral patterns, *ACM Transactions on Graphics*, 2015, 34(6), 172.
[DOI: 10.1145/2816795.2818077]
- [17] **Winslow P., Pellegrino S. and Sharma S.B.,** Mapping two-way grids onto free-form surfaces, *Journal of the International Association for Shell and Spatial Structures*, 2008, 49, 123-130.
- [18] **Lebée, A., & Sab, K.** Homogenization of a space frame as a thick plate: Application of the Bending-Gradient theory to a beam lattice, *Computers & Structures*, 2013, 127, 88-101.
[DOI: 10.1016/j.compstruc.2013.01.011]
- [19] **Winslow, P., Pellegrino, S., & Sharma, S. B.,** Multi-objective optimization of free-form grid structures. *Structural and multidisciplinary optimization*, 2010, 40(1-6), 257-269.
[DOI: 10.1007/s00158-009-0358-4]
- [20] **Mesnil R.,** Structural explorations of fabrication-aware design space for non-standard architecture, PhD Thesis, Université Paris-Est.